NUCLEAR STRUCTURE -- EXPERIMENTAL

SEARCH FOR THE GROUND STATE OF ^{11}N

A. Azhari, T. Baumann, J. A. Brown, M. Hellström[a], J. H. Kelley[b], R. A. Kryger, H. Madani[c], E. Ramakrishnan[d], D. Russ[c], T. Suomijärvi[b], P. Thirolf, M. Thoennessen, and S. Yokoyama

The availability of radioactive nuclear beams has opened up the possibility to study nuclei at and even beyond the proton and neutron driplines. The cross sections for single particle transfer reactions coupled with the detector efficiencies are sufficiently large enough to utilize rather small beam intensities. The lifetimes of nuclei beyond the driplines (unstable with respect to neutron or proton decay) are extremely short ($\sim 10^{-21}$s) and thus can not be measured directly with standard methods.

One of the most interesting exotic decay modes on the proton rich side is the ground-state di-proton emission. In heavy nuclei, proton emission can occur with fairly long lifetimes due to the large Coulomb and angular momentum barriers. However, in the light mass region, both the Coulomb barrier as well as the angular momentum barriers are smaller and thus the lifetimes are extremely short. The most recent investigation of the ground-state decay of ^{12}O established a limit of $< 7\%$ for the contribution of di-proton emission [1]. The decay was consistent with a sequential emission of the two protons. However, this sequential decay depends critically on the intermediate system of ^{11}N. The lowest measured state in ^{11}N is a $p_{1/2}$ state with a decay energy of 2.24 MeV and the $s_{1/2}$ ground state was assumed to be at 1.9 MeV which was deduced from the isobaric mass multiplet equation (IMME) [2,3]. With these values the sequential decay of ^{12}O should be strongly suppressed and the calculated decay width is inconsistent with the measured width of 578 ± 205 keV for ^{12}O [1].

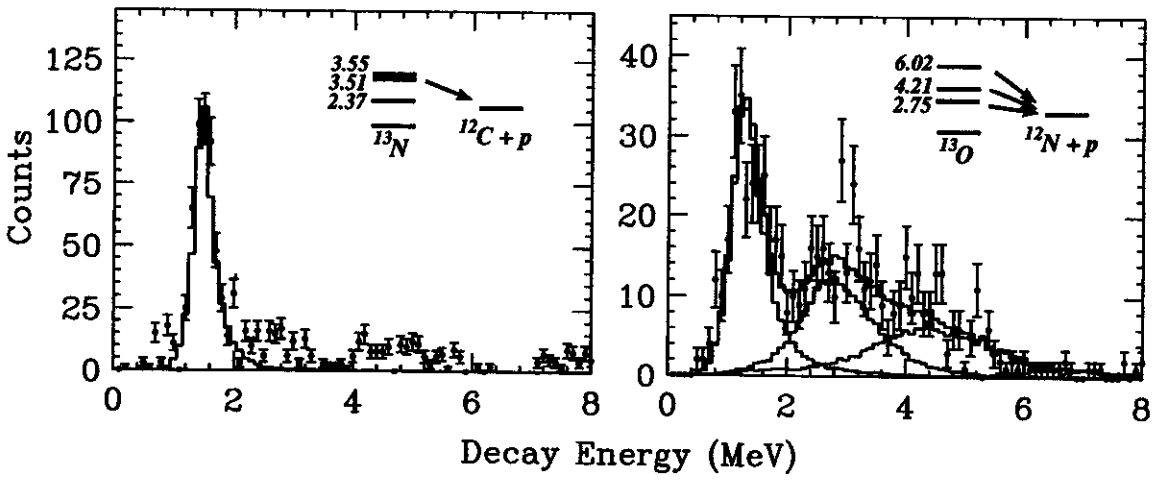

Figure 1: Decay energy spectra for ^{13}N (left) and ^{13}O (right) following the single particle pick-up reaction ^{9}Be(^{12}N,^{13}N) and ^{9}Be(^{12}N,^{13}O), respectively.

Thus, we studied the decay of ^{11}N in order to search for the ground state and determine its decay energy. We used the single neutron stripping reaction ^{9}Be(^{12}N,^{11}N) with a radioactive beam of ^{12}N. This secondary beam was produced from a 80 MeV/nucleon ^{16}O beam and separated in the A1200 and the RPMS velocity filter. The secondary target of 37 mg/cm^2 ^{9}Be was located in front of a telescope consisting of a PPAC, a segmented silicon ΔE detector and a segmented 5mm thick silicon E detector. This telescope was surrounded by a silicon ΔE detector segmented into 16 annular and 16 radial segments which was backed

by 16 plastic phoswich detectors. The efficiency of this arrangement was optimized for decay energies between 1 and 3 MeV [5,6].

In addition to the single neutron stripping reaction populating ^{11}N, the proton decays of unbound states following other transfer reactions were observed. The decay energies and widths of previously measured states were used to calibrate and determine the resolution of the set-up. Figure 1 shows the decay spectra of ^{13}N and ^{13}O following the reactions ^{9}Be(^{12}N,^{13}N) and ^{9}Be(^{12}N,^{13}O) and the corresponding decay schemes.

The decay spectrum of ^{13}N to ^{12}C shows a peak at a decay energy of $\sim$ 1.5 MeV which corresponds to decays of the second and third excited states of ^{13}N which are located at excitation energies of 3.51 MeV and 3.55 MeV with widths of 62 keV and 47 keV, respectively [4]. The decay energy of the first excited state at 2.37 MeV is too small (421 keV) to be detected by the present arrangement.

^{13}O also has no bound excited states and the proton decay of the first three excited states at 2.75 MeV, 4.21 MeV and 6.02 MeV [4] can be seen in the decay-energy spectrum in figure 1. Only the width of the third excited state has previously been determined (1.2 MeV) [4]. The widths of the first two excited states were previously unknown and from a preliminary analysis of the present data, values of 400 keV and 500 keV, respectively, were extracted.

The decay-energy spectrum of ^{11}N is shown in figure 2. It exhibits one broad peak around 2 MeV with a strong asymmetry at lower energies. Assuming that this peak is dominated by the previously measured $p_{1/2}$ state at 2.24 MeV, it is clear that an additional peak at lower energies is necessary in order to fit the data. In the fit shown in figure 2, the 2.24 MeV peak was kept fixed with a width of 740 keV [2]. The low-energy part could be fitted by adding a peak at 1.5 MeV with a width of 2.4 MeV. The data could not be described with one single peak with an intermediate energy.

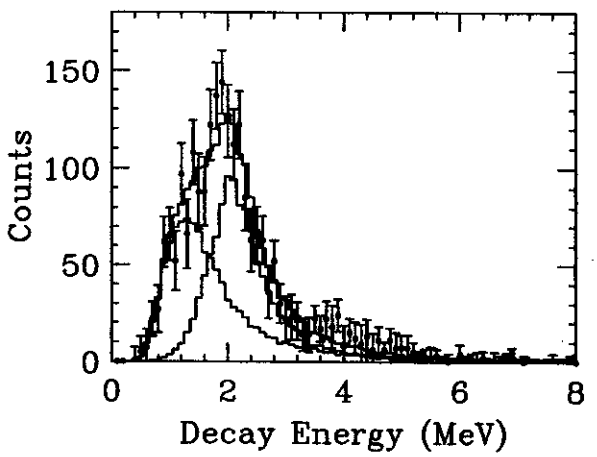

Figure 2: Decay energy spectrum of ^{11}N

Even when the apparent $p_{1/2}$ state was lowered to 2 MeV, an additional component was necessary to fit the data. The detailed values of this peak at low decay energy have to be determined by a χ^2-search including a variation of the upper peak. The present observation of a state $\sim$ 1.5 MeV with a rather broad width is consistent with recent theoretical predictions. A reanalysis of the isobaric analogue states in ^{11}B and ^{11}C by Sherr indicated that the IMME predicts the $s_{1/2}$ state to be located between 1.1-1.5 MeV [7]. H.T. Fortune *et al.* calculated the level structure of ^{11}N using a Woods-Saxon plus Coulomb plus spin-orbit potential [8]. They predict the $p_{1/2}$ state to be at 2.48 MeV, about 200 keV higher than the measured value,

and the $s_{1/2}$ state at 1.60 ± 0.22 MeV excitation energy.

In conclusion, we observed the 2.24 MeV excited state in ^{11}N and evidence for a low lying state, at $\sim$ 1.5 MeV decay energy and a width of $\sim$ 2.4 MeV, was observed. Recent theoretical calculations agree with this new result and the existence of this state at significantly lower decay energy in ^{11}N could also explain the sequential decay nature of the two-proton decay of ^{12}O.

a. Gesellschaft für Schwerionenforshung, D-64220 Darmstadt, Germany.
b. Institut de Physique Nucleaire, IN2P3-CNRS, 91406 Orsay, France.
c. Department of Chemistry, University of Maryland, College Park, Maryland 20742, USA.
d. Cyclotron Institute, Texas A&M University, College Station, TX 77843.

References

1. R. A. Kryger *et al.*, Phys. Rev. Lett. 74, 860 (1995).
2. W. Benenson *et al.*, Phys. Rev. C9, 2130 (1974).
3. F. Ajzenberg-Selove, Nucl. Phys. A506, 1 (1990).
4. F. Ajzenberg-Selove, Nucl. Phys. A523, 1 (1991).
5. M. Thoennessen *et al.*, Proc. of the Int. Conf. on Exotic Nuclei and Atomic Masses, Arles, France, June 19-23 (1995).
6. A. Azhari, *et al.* Annual Report 1994, NSCL/MSU, p. 83 (1994).
7. R. Sherr, private communication.
8. H. T. Fortune, D. Koltenuk and C. K. Lau, Phys. Rev. C51, 3023 (1995).

VIRTUAL PHOTON SCATTERING OF ^{11}Be

N. Gan[a], J. R. Beene[a], M. L. Halbert[a], D. W. Stracener[a], R. L. Varner[a], A. Azhari, J. Brown, D. J. Morrissey, N. T. B. Stone, P. Thirolf[b], M. Thoennessen, G. D. Westfall, and S. Yokoyama

The measurement of the properties of giant resonance (GDR) in cold nuclei has so far been restricted to β-stable nuclei. The recent developement of intense radioactive beams opened up the opportunity to study the GDR in exotic nuclei. The method of virtual photon absorption or photon scattering can be used to excite and detect the GDR in the projectile. Both methods rely on the large Coulomb excitation cross section for high energy beams on high Z targets. In the vitual photon absorption method the projectile excitation energy can be reconstructed by measuring the energy of all the products from the decaying projectile, whereas in virtual photon scattering the γ-ray decay back to the ground state of the projectile is measured.

We attempted to measure the virtual photon scattering of ^{11}Be. Presently the method is limited to a few selected nuclei because of two limitations: (i) the nucleus should not have any bound excited states, and (ii) relatively large beam intensities are not available for the very exotic nuclei like ^{11}Li. Both these problems will be solved with the S800 and the coupling of the two cyclotrons, respectively. ^{11}Be was chosen as the first case because various reactions have been well studied. Breakup reactions on light and heavy targets have been measured by Anne *et al.* [1], and discrete γ-ray measurements have been presented in Reference 2.

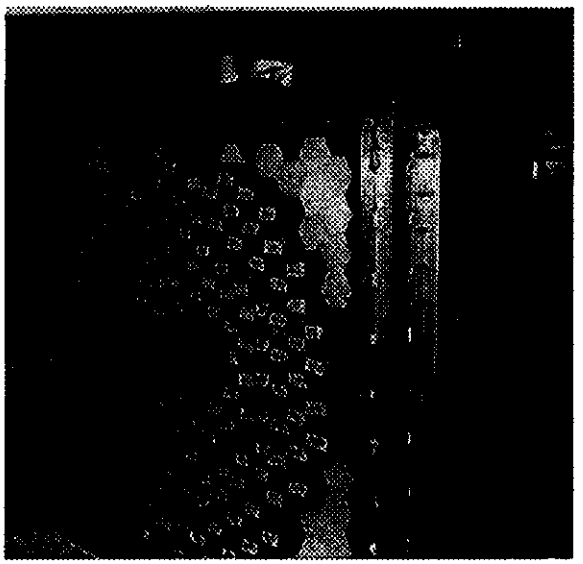

Figure 1: The ORNL-TAMU-MSU BaF_2 Array. The 142 detectors covered forward angles between 12° – 44°. The target is located 45 cm in front of the array the beam pipe and the fragment detector is hidden behind the BaF_2 array.

A 77 MeV/nucleon ^{11}Be beam, produced from the fragmentation of 100 MeV/nucleon ^{13}C on a 940 mg/cm^2 Be production target bombarded an 80 mg/cm^2 thick secondary ^{208}Pb target. The average beam intensity of the ^{11}Be was 10^6 particles/second. The inelastically scattered exotic beam particles were detected in the zero-degree detector from the MSU 4π array [3] covering angles of 0.5 - 1.5° which

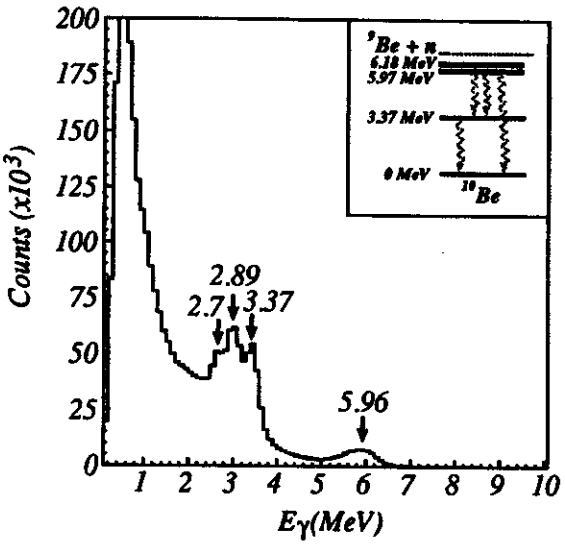

Figure 2: Doppler-corrected γ-ray spectrum in coincidence with ^{10}Be fragments in the forward array following inelastic scattering of ^{11}Be on ^{208}Pb.

was located about 150 cm behind the target. Since ^{11}Be has only one bound state at $\sim$ 300 keV, the identification of a mass 11 ejectile in coincidence with a γ-ray is sufficient to determine a scattering event.

The γ-rays in coincidence with ^{11}Be were detected with the ORNL-TAMU-MSU BaF_2 array. This array consists of 142 large BaF_2 detectors and was placed at a distance of 45 cm from the target surrounding the beam pipe. It covered an angular range of 12° – 44°. Due to the Lorentz boost this corresponded to covereage of 24% of the total solid angle. This was the first experiment with the array and a picture of the setup can be seen in Figure 1. In addition to the large BaF_2 array at forward angles, a small array of seven BaF_2 detectors was located at backward angles in order to measure the contributions from target excitations.

Figure 2 shows the doppler corrected γ-ray spectrum in coincidence with ^{10}Be fragments. Peaks corresponding to the transitions between the bound states of ^{10}Be can clearly be identified. Further analysis including the obtained γ-ray spectra in coincidence with ^{11}Be fragments are currently in progress.

a. Oak Ridge National Laboratory, Operated by Lockheed Martin Energy Res., Oak Ridge, TN 37831.
b. Present address: Technische Universität München, Beschleunigerlaboratorium, 85748 Garching, Germany.

References

1. R. Anne, *et al.* Nucl. Phys. A575, 125 (1994).
2. R. Anne, *et al.* Z. Phys. A, 397 (1995).
3. N. T. B. Stone, *et al.* Annual Report 1994, NSCL/MSU, p. 181 (1994).

MEASUREMENT OF THE REACTION CROSS SECTION OF d(^{7}Be,^{8}B)n AS A STRUCTURE PROBE OF THE ^{8}B NUCLEUS

C. F. Powell, D. J. Morrissey, J. A. Brown, B. Davids, M. Fauerbach,
J. H. Kelley[a], R. Pfaff, and B. M. Sherrill.

A large amount of speculation has been made about the structure of the exotic nucleus ^{8}B. In particular, the possible existence of a single-proton halo in this nucleus has been suggested. Numerous experiments have been performed with ^{8}B, including measurements of total interaction cross section [1], quadrupole moment [2], quasielastic scattering cross section [3], and momentum distributions of the breakup fragments [4]. These studies have reached conflicting conclusions about the existence of a proton halo. We performed NSCL Experiment 93045 in order to study the structure of ^{8}B using a different approach: the measurement of the d(^{7}Be, ^{8}B)n reaction cross section and the determination of the spectroscopic factor for the ground state of ^{8}B.

In order to measure the (d,n) cross section of a reaction involving short-lived isotopes, it is necessary to use inverse kinematics. The NSCL is ideally suited for studies of this type because the A1200 radioactive beam facility can produce intense beams of exotic nuclei. Also, the existence of the NSCL Neutron Time-of-Flight array and a wide array of heavy ion detection equipment allows the measurement to be made with a minimum of detector development.

Because this was the first measurement of its kind at the NSCL, it was important that a similar reaction which has been extensively studied also be measured as a proof-of-technique. The comparison reaction chosen was d(^{12}C,^{13}N)n. This reaction is ideal because it is well-documented over a range of energies [5,6] and the relatively high energy of the first excited state of ^{13}N (2.37 MeV) should allow unambiguous separation of reactions leading to the ground state. Demonstration of the validity of the technique for the d(^{12}C,^{13}N)n reaction would substantiate the measurement of the cross section of d(^{7}Be,^{8}B)n.

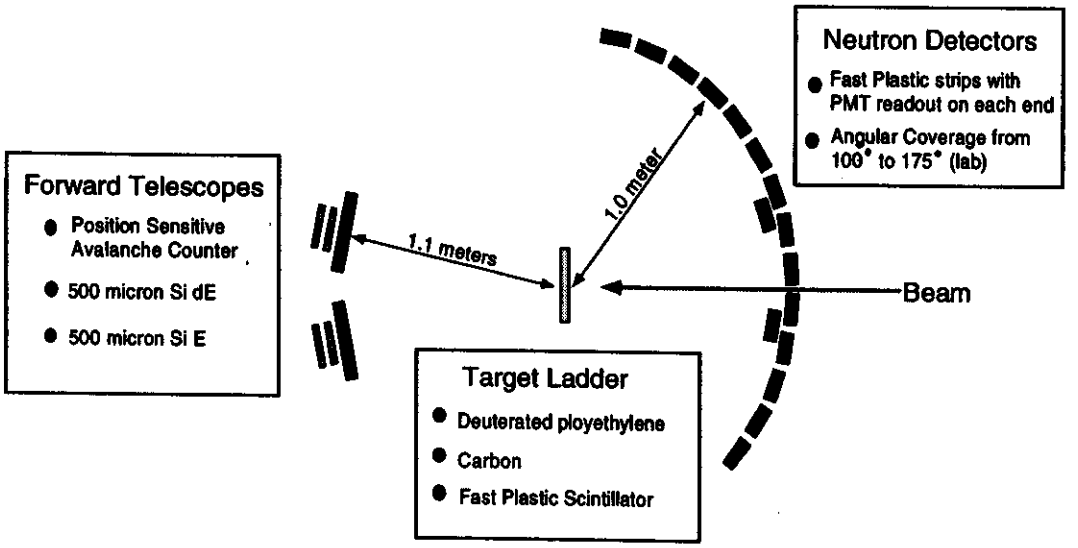

Figure 1: Detector placement for inverse kinematics measurement of the (d,n) cross sections.

The heavy ion beams used in the reaction studies were produced in the A1200 from a primary beam of ^{12}C @ 60 MeV/A. A 790 mg/cm^{2} Be target and 300 mg/cm^{2} Al wedge were used to produce a beam of ^{12}C @ 22 MeV/A. A production target of 587 mg/cm^{2} Be and a 300 mg/cm^{2} Al wedge were

subsequently used to produce the beam of ^{7}Be @ 25 MeV/A. This target-wedge combination gave a ^{7}Be production rate of ~3500 $s^{-1}pna^{-1}$ at the A1200 focal plane, and transfer to the N3 vault produced a loss of ~50%.

The experiment was designed to measure the reaction cross sections of d(^{12}C,^{13}N)n and d(^{7}Be,^{8}B)n in inverse kinematics. Figure 1 shows a schematic of the detectors used to make the measurement. The beam from the A1200 was focussed onto a deuterated polyethylene target. Heavy-ion telescopes measured the angle and energy of the forward products, and the NSCL Neutron TOF array measured the angle and energy of the coincident neutrons emitted in the backward direction. The kinematics curves for these reactions at the specified energies are shown in Figure 2, along with the measured kinematics from experiment 93045. The agreement of these data is quite good, and it is clearly shown that reactions leaving ^{13}N in its first excited state, if they were present in this data, would be resolved.

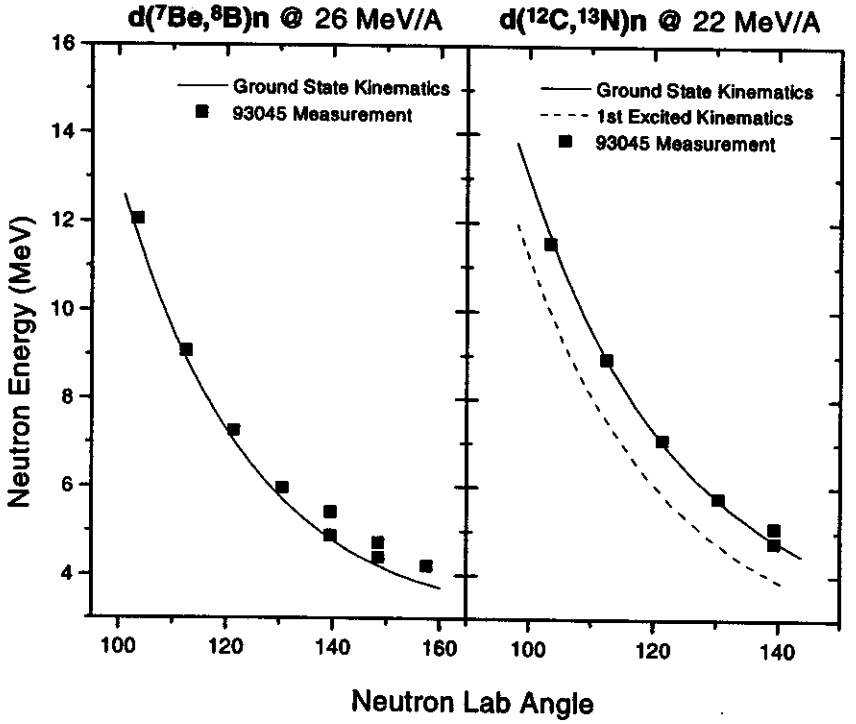

Figure 2: The (d,n) reactions in inverse kinematics

The angular distribution of the cross sections determined from the coincidence events are shown in Figure 3, along with DWBA predictions. Unfortunately, the measurement of the reaction cross sections could only be made over a small range of angles. This was caused primarily by geometric limitations of the 92" scattering chamber which restricted the positioning of the large neutron detector array. In addition, the large physical frame of the parallel plate avalanche counters (used to measure the position of the heavy product) prevented positioning of the forward telescopes at angles very near the beam axis. The combination of these two geometric limitations led to the small angular coverage of the coincidence detector array, which can be seen in Figure 3.

Absolute normalization of beam particles hitting the reaction target was limited by several factors in experiment 93045. At the time of the experiment, the A1200 production target beam-current monitors were not functioning properly. Measurements of the beam current using a beamline faraday cup were thus the only normalization available, which led to an uncertainty in the number of particles on

target of ~30% for the d(^{12}C,^{13}N)n reaction. Lack of an accurate normalization prevented an absolute measurement of the reaction cross sections.

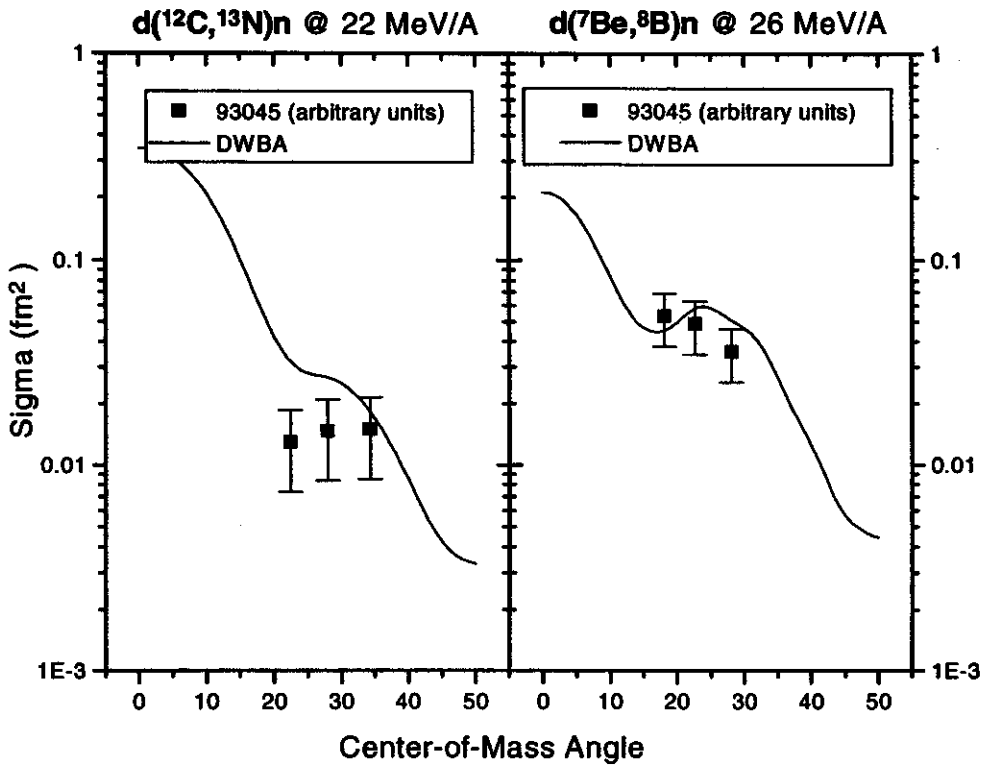

Figure 3. Measured reaction cross sections and DWBA predictions from DWUCK4 [7].

These problems limited the success of experiment 93045, but the experiment clearly demonstrated the feasibility of the measurement of the (d,n) cross section in inverse kinematics. Approved NSCL Experiment 96019 will address the difficulties encountered during 93045. Improvements in the detector arrangement and accurate beam current monitoring will lead to a precise measure of the reaction cross sections over a useful range of angles.

a. Present Address: GANIL, Boite Postale 5027, 14021 Caen Cedex, France.

References

1. I. Tanihata et al., *Phys. Lett.*, **B206** (1988) 592.
2. T. Minamisono et al., *Phys. Rev. Lett.*, **69** (1992) 2058.
3. I. Pecina et al., *Phys. Rev. C*, **52** (1995) 191.
4. W. Schwab et al., Z. *Phys.*, **A350** (1995) 283.
5. H. R. Schelin et al., *Nucl. Phys.*, **A414** (1984) 67.
6. L. M. C. Dutton et al., *Nucl. Phys.*, **A178** (1972) 488.
7. Program DWUCK4, P. D. Kunz (unpublished), Extended version of J. R. Comfort (unpublished).

LIMIT OF THE LIFETIME OF ^{16}B

R. A. Kryger, A. Azhari, J. Brown, J. Caggiano, M. Hellström[a], J.H. Kelley[b],
B.M. Sherrill, M. Steiner, and M. Thoennessen

The exact location of the driplines is one of the most stringent tests of nuclear structure models. Whereas the proton dripline can be measured and studied up to very heavy nuclei, the neutron dripline is currently inaccessible beyond Z $\sim$ 8 [1,2]. The possibility to observe neutron radioactivity along the dripline relies solely on the (small) angular momentum barrier and is extremely difficult because of the very short lifetimes.

One possible case is ^{16}B where the last neutron probably populates a $d_{5/2}$ state. ^{16}B is known to be particle unstable because it was not observed in the spallation of uranium with 4.8 GeV protons [3] nor in the fragmentation of ^{40}Ar at 44 MeV/nucleon [4]. From the length of the flight path and the velocity of the fragments an upper limit on the lifetime of 9 ns can be extracted. On the other hand, a recent measurement of the multiple transfer reaction ^{14}C(^{14}C,^{12}N)^{16}B found a state very close to the threshold at 40$\pm$60 keV [5]. Assuming a width of <100 keV results in a lower limit on the lifetime of $> 6.6 \cdot 10^{-21}$s.

Simple shell model calculations predict ^{16}B to have a lifetime of $3.7 \cdot 10^{-16}$s and $1.1 \cdot 10^{-13}$s for decay energies of 10 keV and 1 keV, respectively, assuming a $d_{5/2}$ configuration. Thus, the range of possible lifetimes is quite large and extremely difficult to measure.

In a first attempt, we tried to lower the limit of the present experimental range from the long-lived side by designing an experiment similar to the fragmentation measurements. The significantly reduced time-of-flight, compared to the previous measurements, allowed a reduction on the upper limit of the life time. We used a single proton stripping reaction from a radioactive beam of ^{17}C to produce ^{16}B. Fragment separation following this reaction was not necessary due to the small background. The radioactive ^{17}C beam was produced via fragmentation of 80 MeV/nucleon ^{18}O and then selected with the A1200 fragment separator at the NSCL. A ΔE silicon detector in front of the secondary 114 mg/cm^2 thick carbon target coupled with the flight time through the A1200 allowed the identification of the ^{17}C isotopes. Directly after the target a ΔE-ΔE-ΔE-E telescope with thicknesses of 303 μm, 498 μm, 5 mm and 5 mm stopped the beam and the reaction products. The distance between the secondary target and the E detector was only 5 cm. Further experimental details can be found in Ref. [6].

The setup was tested with the reaction ^{nat}C(^{16}C,^{15}B). Figure 1 shows the particle identification

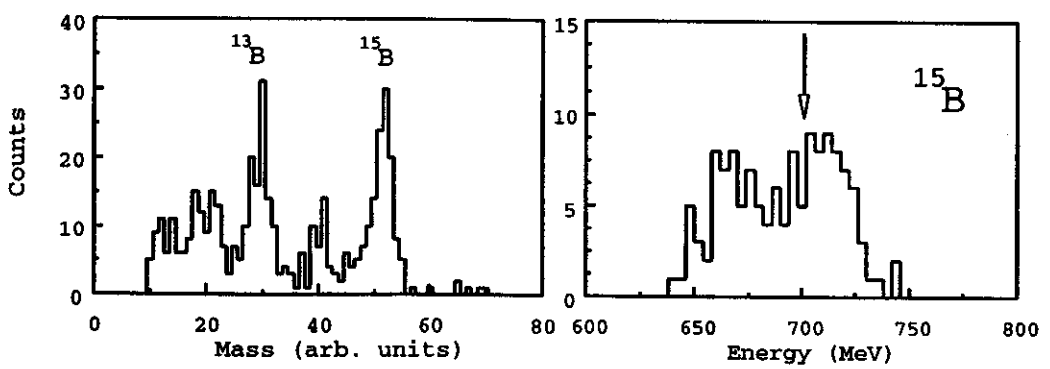

Figure 1: Isotope identification spectrum (left) and energy spectrum for ^{15}B (right) following proton stripping reactions from a ^{16}C beam.

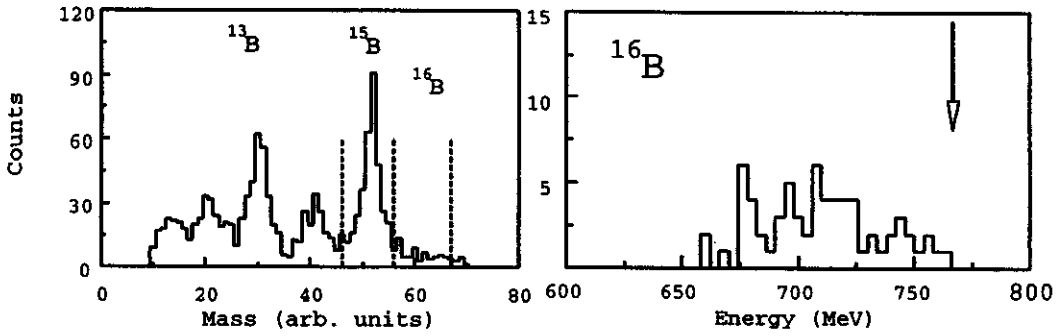

Figure 2: Isotope identification spectrum (left) and energy spectrum for ^{16}B (right) following proton stripping reactions from a ^{17}C beam.

(left) and the energy spectrum of the ^{15}B fragments (right) which resulted from the one proton stripping reaction. The arrow corresponds to pure fragmentation reactions where the fragments continue with the initial ^{16}C beam velocity corrected for energy loss in the target. The peak due to the transfer reaction ^{12}C(^{16}C,^{15}B)^{13}N would be $\sim$ 20 MeV higher. The observed broad peak between these two energies suggests that both reaction types contribute.

The corresponding spectra for the reaction ^{nat}C(^{17}C,^{16}B) is shown in Figure 2. The absence of a ^{16}B peak in the left part of the figure confirms that ^{16}B is unbound. The right part of Figure 2 shows the energy spectrum of the 67 (background) events which appear in the ^{16}B gate of the particle spectrum. Most of the events are at much lower energies compared to the arrow indicating fragmentation events. Only 4 events still qualify when an additional gate on the energy is applied. The ^{15}B (Figure 2, left) spectrum from the ^{17}C fragmentation actually shows a peak at the same position as in the ^{16}C reaction (Figure 1, left) indicating that these events are predominantly due to one-proton stripping followed by neutron decay [6]. Using the measured cross section for these reactions and assuming that the four events in the energy gated ^{16}B window are indeed ^{16}B, a new upper limit of 191 ps for the life time of ^{16}B was extracted. Although this is a factor of $\sim$ 50 smaller than the previous value, it narrows the possible window of lifetimes only by a small fraction. The exact determination of the ^{16}B lifetime therefore remains a major experimental challenge.

a. Present address: Gesellschaft für Schwerionenforschung, D-64220 Darmstadt, Germany.
b. Present address: Institut de Physique Nucleaire, IN2P3-CNRS, 91406 Orsay, France.

References

1. D. Guillemaud-Mueller *et al.*, Phys. Rev. C41, 937, (1990).
2. M. Fauerbach, D. J. Morrissey, W. Benenson, B. A. Brown, M. Hellström, J. H. Kelley, R. A. Kryger, R. Pfaff, C. F. Powell, and B. M. Sherrill, Phys. Rev. C53, 647, (1996).
3. J. D. Bowman, A. M. Poskanzer, R. G. Korteling, and G. W. Butler, Phys. Rev. C9, 836 (1974).
4. M. Langevin *et al.*, Phys. Lett. 150B, 71 (1985).
5. H. G. Bohlen *et al.*, Nucl. Phys. A583, 775c (1995).
6. R. A. Kryger, A. Azhari, J. Brown, J. Caggiano, M. Hellström, J. H. Kelley, B. M. Sherrill, M. Steiner and M. Thoennessen, Phys. Rev. C53, in press (1996).

GROUND STATE OF ^{10}Li

S. Yokoyama, A. Azhari, T. Baumann[a], J. Brown, A. Galonsky, P. G. Hansen, J. H. Kelley[b], R. A. Kryger, R. Pfaff, E. Ramakrishnan[c], P. Thirolf[d], and M. Thoennessen

The detailed knowledge of the properties of the ^{10}Li ground state is crucial for the understanding of the halo nucleus ^{11}Li. Several experiments found evidence for a low lying *s*-wave state in ^{10}Li [1-3]. However a recent multiple nucleon transfer experiment observed a *p*-wave state at 240 keV [4]. We improved the energy resolution of the experimental setup by Kryger *et al.* [1] in order to set more stringent limits on the resonance peak values.

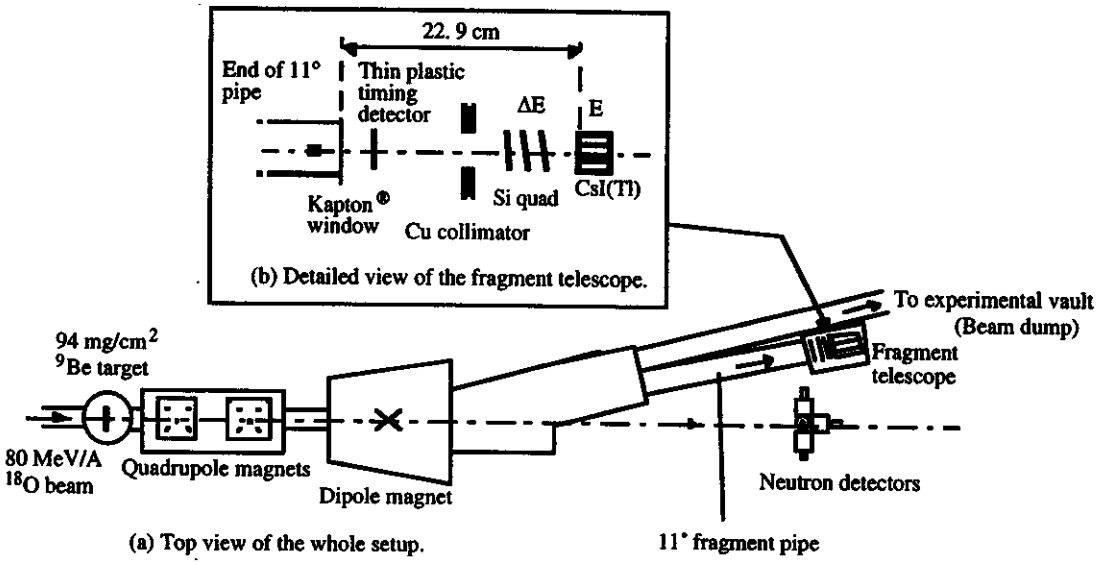

Fig. 1: Schematic diagram of the fragment telescope.

The ground state of ^{10}Li was studied with the method of sequential neutron decay spectroscopy at 0°. The ^{10}Li nuclei were produced in the fragmentation of an 80 MeV/nucleon ^{18}O primary beam from the K1200 cyclotron at the NSCL on a 94 mg/cm^2 ^{9}Be target. After the target, the primary beam and the fragmentation products were separated from the neutrons with a set of quadrupole magnets and a dipole magnet. The ^{9}Li fragments and other A/Z = 3 fragments (^{6}He, ^{12}Be and ^{15}B) were detected in a silicon CsI(Tl) telescope at the end of a beam pipe 11° from the incident primary beam axis. The neutrons were measured with an array of five NE213 liquid scintillator detectors at the distance of ~ 5.8 m from the target (Fig. 1 (a)). The resonance energy E_r of ^{10}Li was calculated from the relative velocity,

$$E_r = \frac{1}{2}\mu v_{rel} \qquad (1)$$

where μ is a reduced mass of a ^{9}Li and a neutron system and where the relative velocity v_{rel} (= v_n - v_f) was derived from the neutron (v_n) and fragment (v_f) velocities.

One main improvement compared to the previous experiment was the fragment detector. Fig. 1 (b) shows a schematic of the fragment telescope which consists of three-quadrant segmented ΔE silicon detectors and nine CsI(Tl) E detectors instead of a plastic phoswich ΔE-E detector arrangement. The fragment velocity was deduced from the energy and not from the TOF. The energy resolution of the CsI(Tl) E detectors were ~ 0.7%. This translates to a TOF resolution of σ = 0.057 ns compared to the

resolution of σ = 0.89 ns of the previous experiment.

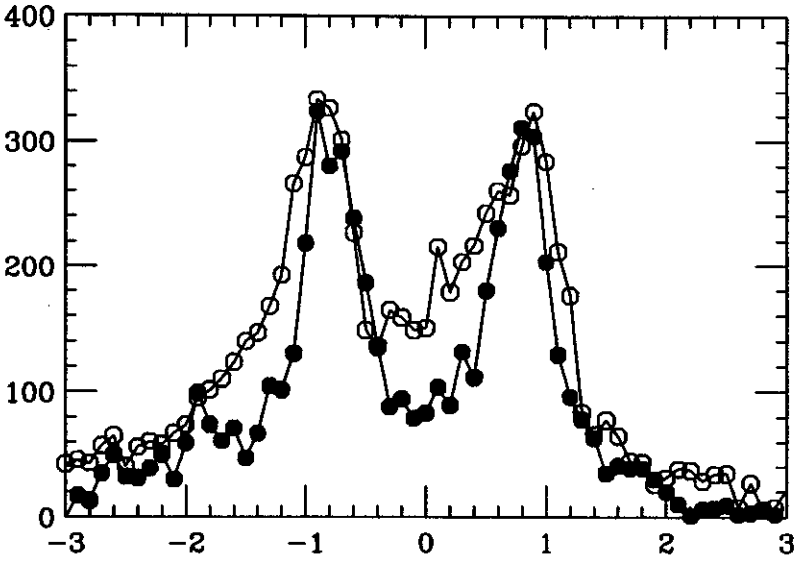

Fig. 2: Comparison of the relative velocity spectrum of the neutron decay of ^{7}He for the previous experiment [1] and the current work. Dark circles represent the current data and white circles are the old data. They are connected with straight lines for a comparison. The old data peak heights are normalized to the new data.

The new method also allowed us to improve the neutron TOF measurement. In the previous experiment it was measured with respect to the RF signal of the K1200 cyclotron which had a resolution of σ = 0.89 ns in the time of flight of neutrons. Now we timed the neutrons relative to the fragments. This relative timing, together with the calculated fragment TOF (derived from the energy) enabled us to calculate the TOF of the neutrons. This method improved the time resolution of the neutron TOF to σ = 0.70 ns.

Fig. 2 shows this improvement in terms of the relative velocity spectra of ^{7}He decay, to ^{6}He and a neutron, for the previous experiment and the current work. This reaction was used as a calibration of the method since the resonance energy (E_r = 440 keV) and the width (Γ_0 = 160 keV) of the ^{7}He nucleus has been well established [5].

The energy and width of the ^{10}Li ground state were extracted via Monte Carlo simulations. A Breit-Wigner line shape of the form [6]

$$\frac{d\sigma}{d\Omega} \propto \frac{\Gamma(E)}{(E-E_r)^2 + \frac{1}{4}[\Gamma(E)]^2} \qquad (2)$$

where

$$\Gamma(E) = \frac{kP_l(E)}{k_r P_l(E_r)}\Gamma_0 \qquad (3)$$

and is the l-dependent neutron penetrability function, was used for the calculation.

Fig. 3 shows the data and one of the calculations for the relative velocity spectrum of ^{9}Li in coincidence with a neutron. The data are dominated by a single peak near 0 cm/ns as the previous experiment [1]. Two small side peaks which were not so obvious in the previous data, are also observed in the spectrum. These side peaks can be fitted rather well with the parameters for a p-wave (l = 1, E_r = 538 keV, Γ_0 = 358 keV) as reported by Young *et al.* [2].

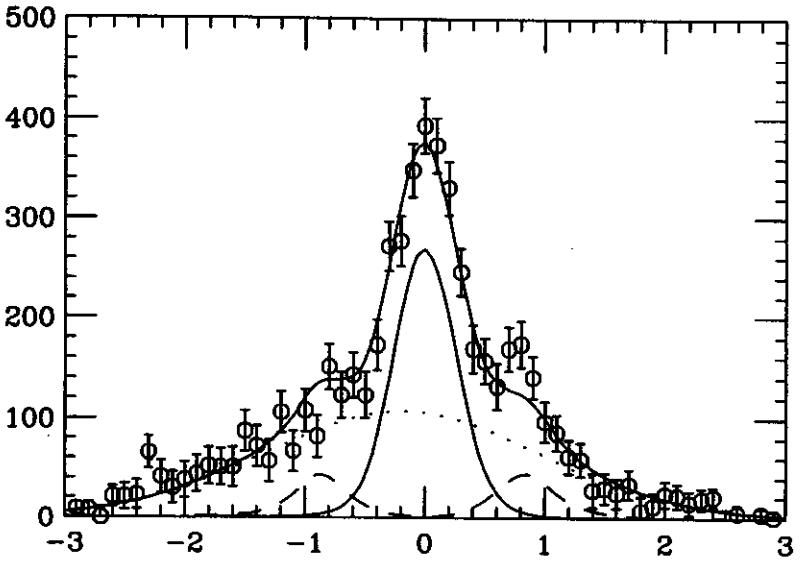

Fig. 3: Relative velocity spectrum and Monte Carlo simulation of ^{10}Li neutron decay. Dotted line and dashed line show estimated Gaussian background and *p*-wave resonance reported by Young *et al.* respectively. Lower solid line shows a Monte Carlo simulation of the *s*-wave state with E_r = 50 keV and Γ_0 = 100 keV. Upper solid line is a sum of the other lines.

The ground state of ^{10}Li could either have a 1*s* or 2*p* valence neutron. Calculated and measured relative velocity spectra were compared using a test in the range from -3.0 cm/ns to 3.0 cm/ns. The condition was used to decide our limits on the decay energy and the width of ^{10}Li ground state. The Wigner limit was also considered as an upper limit of the width for a each possible resonance energy.

If the ground state of ^{10}Li is a p-wave, the resonance energy of ^{10}Li cannot be larger than E_r = 79 keV. This condition rules out the possibility that the central peak we observed is a same state as the one Ostrowski *et al.* observed [4].

For an s-wave, a maximum resonance energy is E_r = 752 keV. At this resonance energy, the width is Γ_0 = 3.84 MeV.

A recent publication [3] suggested a different approach by using the scattering length to describe the s-wave ground state of the ^{10}Li nucleus rather than the Breit-Wigner formula (eq. 2). The analysis to extract the neutron *s*-wave scattering length of ^{9}Li is presently in progress.

a. Present address: Gesellschaft für Schwerionenforschung, D-64220 Darmstadt, Germany.
b. Present address: Institut de Physique Nucleaire, 91406 Orsay CEDEX, France.
c. Present address: Cyclotron Laboratory, Texas A&M University, College Station, TX 77843.
d. Present address: Technische Univ. München, Beschleunigerlaboratorium, 85748 Garching, Germany.

References

1. R. A. Kryger *et al.*, Phys. Rev. C**47**, R2439 (1993).
2. B. M. Young *et al.*, Phys. Rev. C**49**, 279 (1994).
3. M. Zinser *et al.*, Phys. Rev. Lett. **75**, 1719 (1995).
4. A. N. Ostrowski *et al.*, Proceeding of Conf. on Exotic Nuclei and Atomic Masses, Arles, France (1995) to be published.
5. F. Ajzenberg-Selove, Nucl. Phys. A**490**, 1 (1988).
6. A. M. Lane and R. G. Thomas, Rev. Mod. Phys. **30**, 257 (1958), See Sec. XII.3.

ISOVECTOR SPIN STRENGTH IN ^{40}Ca MEASURED BY THE (^{7}Li,^{7}Beγ) REACTION

J.S. Winfield,[a,b] G.M. Crawley, D. Beaumel,[a] S. Danczyk,[c] S. Galès,[a] S.E. Hirzebruch,[a] H. Laurent,[a] I. Lhenry,[a] J.M. Maison,[a] J.C. Staško,[d] and T. Suomijärvi[a]

Although giant resonances have provided abundant information about the nucleus, it is only recently that isovector (ΔT=1) modes of excitation have been studied beyond the well-known giant dipole and Gamow-Teller resonances. The spin response of the continuum at high excitation energy has been even less thoroughly investigated. A discrepancy has arisen recently concerning the nuclear spin excitation of this continuum. Glashausser *et al.* have measured inelastic proton scattering on ^{40}Ca with polarised protons at a bombarding energy of 319 MeV, and found that spin transfer (ΔS=1) transitions are significantly enhanced compared to non-spin transfer (ΔS=0) transitions at excitation energies between 20 and 40 MeV [1]. This enhancement can to a large extent be explained in terms of a model [2] of the response of a semi-infinite slab of interacting particles, and as such is not expected to be associated with a specific target. However, a subsequent measurement by Nakayama *et al.* of spin transfer strength for a ^{12}C target has found that at high excitation energies ΔS=0 transitions are equal to, if not stronger than, ΔS=1 transitions [3]. This latter experiment used the (^{7}Li,^{7}Beγ) reaction at E/A = 26 MeV.

One possible explanation of the discrepancy is that the $(\vec{p},\vec{p}')$ reaction may be dominated by isoscalar excitations, whereas (^{7}Li,^{7}Be) is necessarily isovector. Another possibility is that while in the $(\vec{p},\vec{p}')$ case there is a dominant contribution to the continuum from quasi-free charge exchange, in the heavy-ion reaction a larger contribution is expected from three-body processes. In any case, target-dependent effects could complicate a comparison between ^{40}Ca and ^{12}C. To help clarify the situation, we have performed the (^{7}Li,^{7}Be γ) reaction on the same target nucleus as used in the inelastic proton scattering experiment. We have also used a higher bombarding energy than used by Nakayama *et al.*, which leads to the linear momentum transfer, q, being more closely matched to that of the small to medium angle $(\vec{p},\vec{p}')$ data, where the spin transfer enhancement was most pronounced.

An E/A = 70.4 MeV ^{7}Li beam from the K1200 cyclotron was used to bombard targets of ^{nat}C (3.1 mg/cm^2) and ^{nat}Ca (10.4 mg/cm^2). Scattered ^{7}Be particles were detected by the A1200 magnetic analyser operated as a 0° spectrometer, with the target at what is normally the second dispersive image. The momentum dispersion in this mode of operation is roughly 1.6 cm/% ($\delta p/p$). The maximum angle accepted in the laboratory frame was roughly 1.6°.

At the focal plane, a 7-cm long, 1-mm thick silicon position-sensitive detector (PSD) measured the particle rigidity. The energy-loss signal from the PSD together with the light output from a backing plastic scintillator was used for particle identification. A two-dimensional (X-Y) position-sensitive cathode readout drift chamber mounted close to the silicon detector and another mounted 30 cm in front of it were used to measure the angles of particles at the focal plane event-by-event.

The calcium target was prepared and transported to the chamber with care to avoid oxidation. Despite this, a considerable yield is observed from the reaction on hydrogen on the target (the amount of hydrogen is about 5 μg/cm^2). The likely sources of this hydrogen are from unevaporated hexane solvent, or from incompletely removed oil after the rolling process. The tail of the hydrogen peak obscures the ^{40}K ground state region. However, this region was not of direct interest in the present work.

An array of ten (3 × 3)-cm^2 CsI scintillators, read by photomultipliers, was arranged around the

target at a distance of approximately 5 cm. Stacks of absorbers, consisting of 1-mm each of aluminium, copper and lead, were attached to the front of the scintillators to absorb X-rays and low-energy γ-rays. The CsI detectors and associated amplifiers were calibrated both before and after the beam time with ^{60}Co and ^{137}Cs sources.

The ^{40}Ca(^{7}Li, ^{7}Be)^{40}K singles spectrum is shown in Fig. 1. We observe two resonance-like features in the spectrum: a small enhancement GR1 at roughly 7 MeV excitation energy in ^{40}K, and a broad bump GR2 centered at roughly 11 MeV excitation energy in ^{40}K. A double-Gaussian fit has been made to the region of the two resonances, after subtraction of a smooth background of an assumed continuum. The centroid (in the equivalent ^{40}Ca system) of the fitted Gaussian to GR1 is 15.0 ± 0.5 MeV with a width (corrected for the experimental resolution of 1.5 MeV) $\Gamma_{GR1} = 0.98 \pm 0.4$ MeV. The centroid for GR2 is 18.9 ± 0.8 MeV with $\Gamma_{GR2} = 3.8 \pm 0.8$ MeV. The centroids and corrected widths agree with those of resonances assigned as the isovector octupole (IVOR) and giant dipole (GDR), respectively, in a study of the (^{7}Li, ^{7}Be) reaction on target nuclei ranging from ^{12}C to ^{48}Ti [4]. The identity of resonance GR1 is not obvious from the singles spectrum alone. Although Nakayama *et al.* [4] have assigned it to the IVOR, a collective 2^- state in this region has also been reported in (p, n) and (^{3}He, t) studies [5]. As shown below, we find almost no ΔS=0 strength in this excitation energy region, which supports the 2^- assignment.

In the coincidence analysis, the Doppler-shifted 430 keV γ-rays were identified for each CsI detector from plots of E_γ vs. T_γ. Gates were set on the prompt coincidence time peaks, and also on random time peaks (which were less than 3% of the prompt) for later subtraction. Figure 2 shows a selection of projected γ-energy spectra for CsI detectors at different angles, obtained with the calcium target. The 430-keV peak is prominent in all detectors. Most of the counts on the low-energy side of the peak may be attributed to escaping Compton-scattered photons. While there were few counts on the high-energy side of the peak in the case of the carbon target, this was not the case for the calcium target. This background presumably arises from target de-excitations. From the number of counts in regions of the same width as the 430 keV gate, the γ-background in coincidence with ^{7}Be particles in the focal plane, but *excluding* the region of the hydrogen peak, was estimated as $21 \pm 5\%$ of the 430 keV peak.

The CsI photopeak efficiency, which is required in order to normalise the ^{7}Be$_1$ spectrum, was estimated from the number of counts in the ^{12}B$_{g.s.}$ (1^+) peak in the coincidence spectrum relative to the corresponding number in the singles spectrum. From the relations in Ref. [3], the cross sections for $\sigma(\Delta S{=}0)$ and $\sigma(\Delta S{=}1)$ were constructed. Finally, the "relative strength of spin transfer excitations",

$$P_{sf} = \frac{\sigma(\Delta S=1)}{\sigma(\Delta S=0) + \sigma(\Delta S=1)}$$

was calculated. For unnatural parity transitions the value of P_{sf} should be unity.

The spin strength analysis for the high excitation continuum of the ^{12}C target gives $P_{sf} = 0.44 \pm 0.03$. This agrees with the conclusion of Ref. [3] that the ΔS=0 strength is roughly equal to the ΔS=1 strength at high excitation energy.

The spin strength analysis for the ^{40}Ca target is shown in Fig. 3. Beyond the region of the hydrogen peak, one sees a dramatic rise in the value of P_{sf} at around 6 MeV excitation energy. This appears to be a result of the almost complete cancellation of the singles and coincidence yield to give negligible ΔS=0 strength at this excitation energy [Fig. 3(a)]. The absence of ΔS=0 strength includes the region of the resonance GR1 observed in the singles spectrum, which suggests the assignment of 2^- rather than 3^- for

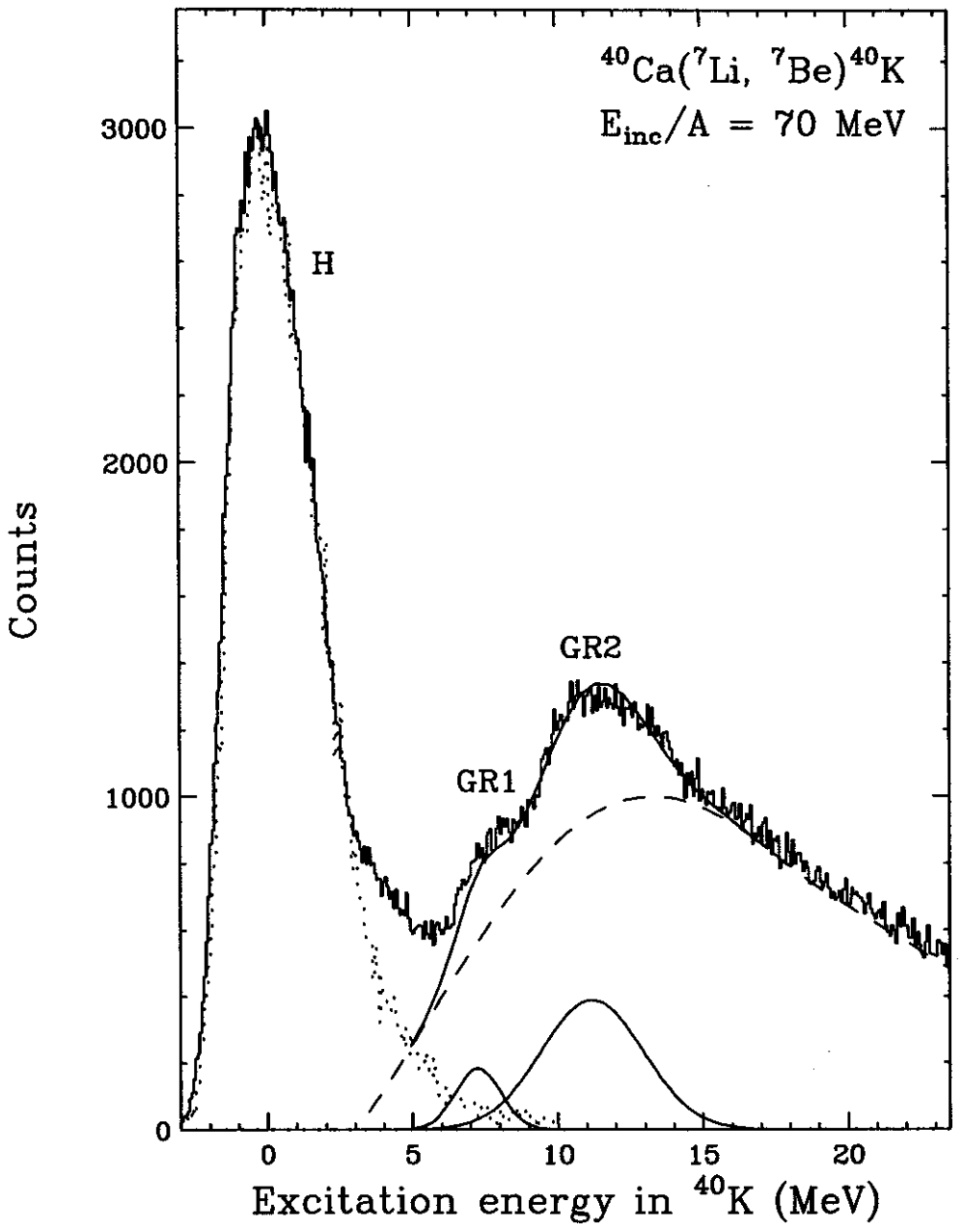

Figure 1: Focal plane singles energy spectrum for the (^{7}Li, ^{7}Be) reaction on ^{40}Ca. The dotted histogram is the hydrogen peak observed with the same reaction on a mylar target. The smooth dashed curve shows the assumed shape of the underlying continuum. The fitted Gaussians to the resonances labelled GR1 and GR2 are described in the text.

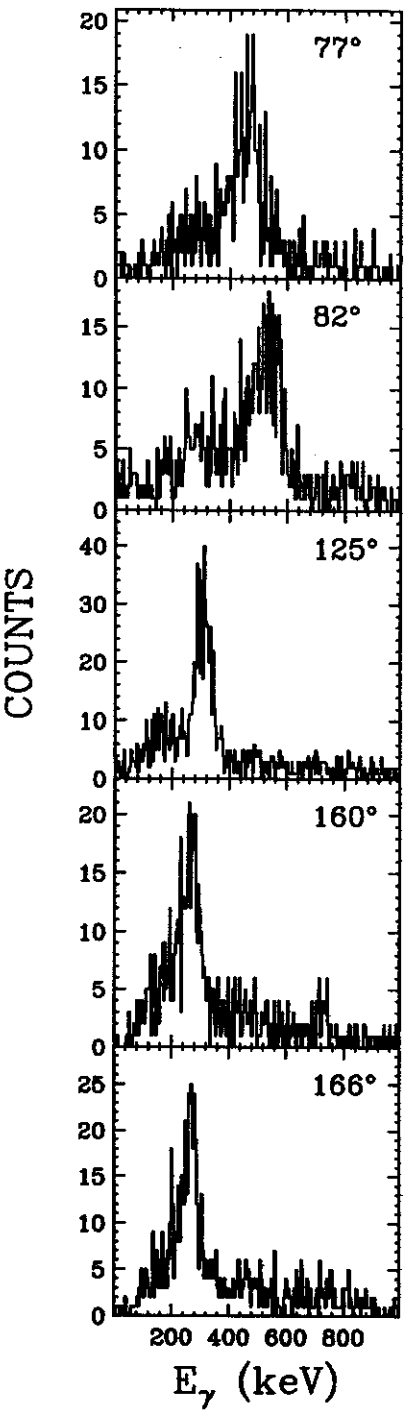

Figure 2: Gamma-ray energy spectra gated on true coincidences with ^{7}Be in the focal plane. Spectra from five sample CsI detectors at different angles to the beam are shown (with the convention that angles less than 90° are forward with respect to the beam).

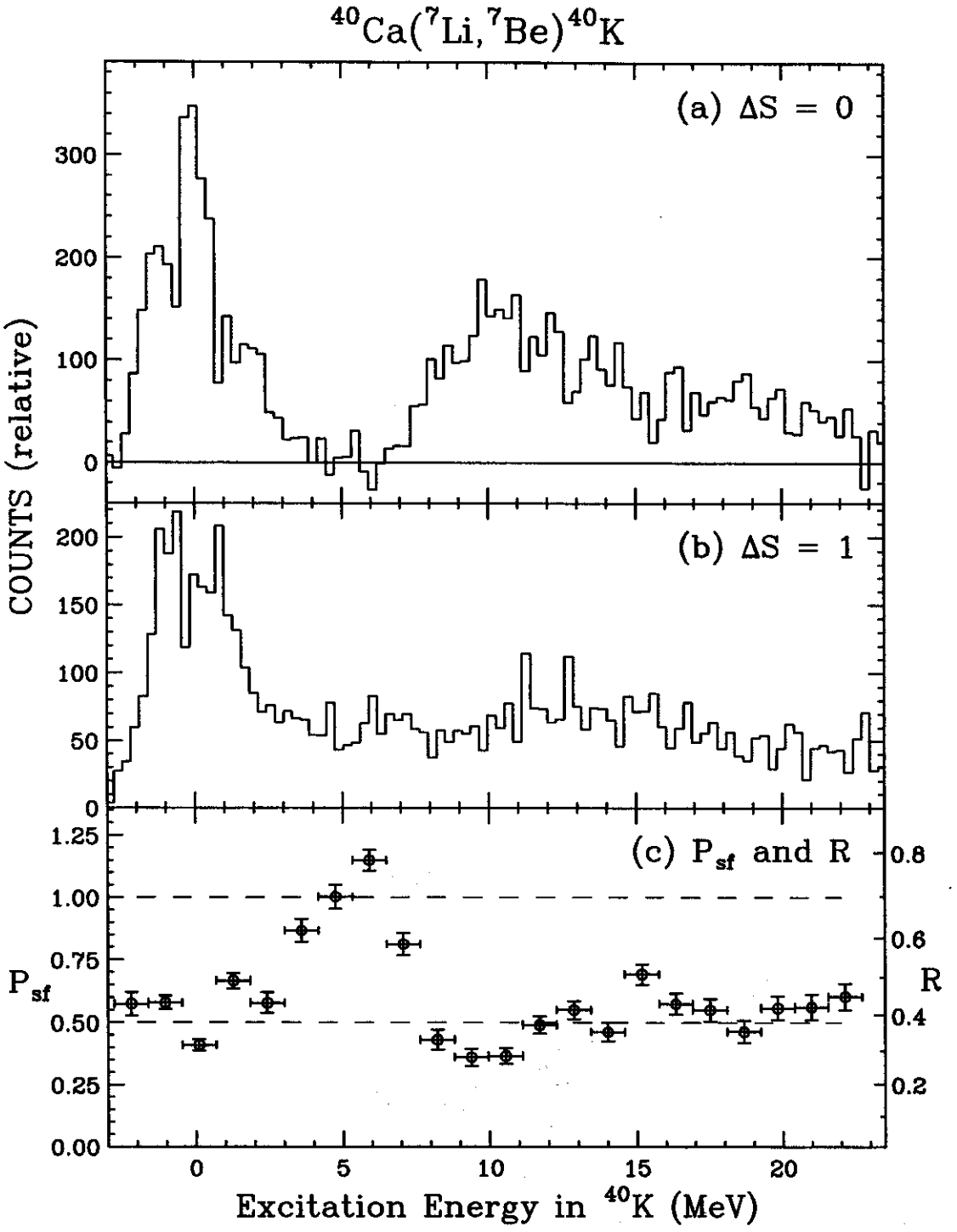

Figure 3: Extracted energy spectra for (^{7}Li,^{7}Be) on ^{40}Ca at $\theta_L \approx 0°$ and $E/A = 70$ MeV for the (a) non-spin transfer and (b) spin transfer channels, and (c) the relative strength of spin excitations. The horizontal bars on the data points in panel (c) indicate the range of averaging over excitation energy. The vertical bars represent statistical errors only.

this resonance, as discussed previously. One observes considerable ΔS=0 strength from roughly 9 MeV to 13 MeV excitation energy in ^{40}K, which covers the region of the GDR analogue seen in the singles spectrum. Indeed, the GDR is well-known to be mainly non-spin transfer. Above 13 MeV excitation in ^{40}K the ΔS=0 strength begins to fall and there is a corresponding small increase in P_{sf}. The average value of P_{sf} is 0.54 ± 0.02 from 17 to 22 MeV excitation in ^{40}K (roughly 25 to 30 MeV excitation in ^{40}Ca). Thus it appears that the high excitation region for the ^{40}Ca target does have somewhat more ΔS=1 strength than that for the ^{12}C target. On the other hand, we do not observe such an outstanding rise in spin strength with increasing excitation energy as seen in the $(\vec{p},\vec{p}')$ experiment.

In summary, following the systematic study of Nakayama *et al.* [4], the (^{7}Li,^{7}Be) reaction has again been shown to be a useful tool to investigate isovector giant resonances. The γ-coincidence technique has been applied to measure the spin transfer strength, particularly in the high excitation continuum. Although somewhat more spin transfer strength lies in the continuum for the calcium target than for carbon, the main conclusion is that there is no significant increase compared to that observed in the $(\vec{p},\vec{p}')$ experiment, since the value of P_{sf} is close to one half. The remaining discrepancy between (^{7}Li,^{7}Be) and $(\vec{p},\vec{p}')$ must then be explained by differing features of the light-ion and heavy-ion reaction mechanisms in the region of the continuum.

a. Institut de Physique Nucléaire, IN_2P_3-CNRS, 91406 Orsay Cedex, France
b. Present address: GANIL, B.P. 5027, 14021 Caen Cedex, France.
c. Present address: Department of Mechanical Engineering, Texas A&M University, College Station, Texas 77843.
d. Present address: Ford Research Laboratory, MD#3429, 2000 Rotunda Drive, Dearborn, Michigan 48121.

References

1. C. Glashausser, *et al.*, Phys. Rev. Lett. 58, 2404 (1987).
2. H. Esbensen and G. Bertsch, Ann. Phys. 157, 226 (1984), and Phys. Rev. C 34, 1419 (1986).
3. S. Nakayama, *et al.*, Phys. Rev. Lett. 67, 1082 (1991); S. Nakayama, *et al.*, Nucl. Phys. A538, 627c (1992).
4. S. Nakayama, *et al.*, Phys. Lett. B 195, 316 (1987).
5. D.J. Horen, *et al.*, Phys. Lett. B 99, 383 (1981); S.Y. van der Werf, *et al.*, J. Phys. (Paris) C 4, 471 (1984).

MEASUREMENT OF THE HALF-LIFE OF ^{108m}Ag

E. B. Norman[a], E. Browne[a], A. J. Smith[a], R. J. McDonald[a], M. Fauerbach, P.F. Mantica, D.J. Morrissey, R. Pfaff, C.F. Powell, M. Steiner

^{108m}Ag has been proposed as a γ-ray standard for calibrating energies and absolute efficiencies of germanium detectors [1] for the following reasons:

- Its γ-ray energies and absolute intensities are well known [1,2]
- It can be easily produced by the ^{107}Ag(n,γ) reaction
- It has a long half-life (127-418 years)

For calibrating absolute efficiencies, however, the isotope's half-life should be accurately known in order to correct for decay the activity of the standard source as needed. Ideally, for a standard source that lasts 5 half-lives or 15 years, whichever is shorter, the uncertainty in its activity due to the half-life should be no more than 0.1%. Unfortunately this is not the case with ^{108m}Ag, for which the following discrepant set of values has been reported:

- 127±7 yr. [4]
- 310±132 yr. [5]
- 418±15 yr. [6]

Obviously, a new measurement is needed to resolve this discrepancy. The half-life of ^{108m}Ag can be determined by measuring the activity of the isotope from a source that contains a known number of ^{108m}Ag atoms. We produced the ^{108m}Ag source by fragmenting a ^{109}Ag beam, mass-separating ^{108}Ag, and implanting a known number of these fragments into a 1 mm-thick Al foil.

A 55 MeV/nucleon ^{109}Ag beam from the K1200 cyclotron of the National Superconducting Cyclotron Laboratory at Michigan State University bombarded a 47mg/cm^2 ^{9}Be target at the medium acceptance target position of the A1200 fragment separator [7]. The momentum acceptance of the A1200 separator was limited to ±0.125%, and the angular acceptances were ±10 mrad in θ, and ±20 mrad in ϕ. Since both ^{108}Ag (2.4 min) and ^{108m}Ag were produced by the bombardment, the experimental setup slightly deviated from the usual A1200 focal-plane setup. We placed a HPGe detector (120% efficiency) close to the Al implantation foil to measure the 633-keV γ ray emitted by ^{108}Ag (2.4 min.) and thus determine the number of ^{108}Ag (2.4 min.) fragments that reached the focal plane. Figure 1 shows the γ-ray spectrum measured (for about 24 hours) during implantation.

A three-element silicon E-ΔE detector telescope (100-100-1000 mm thick) periodically monitored the fragments and measured the total number that reached the focal plane of the A1200 fragment separator. From this result it is possible to determine the total number of ^{108}Ag(2.4 min.) + ^{108m}Ag fragments . An aperture (which covered 300 mm^2, the same area of the Si telescope detector) placed against the Al foil ensured fragment implantation on an area equal to that of the Si telescope detector, and thus provided a correct measurement of the number of implanted fragments. The difference between the number of ^{108}Ag (2.4 min.) + ^{108m}Ag fragments (measured with the Si telescope detector), and the number of ^{108}Ag (2.4 min.) fragments (determined by the γ-ray measurement), gives the number of ^{108m}Ag fragments implanted on the Al foil.

The beam current was constantly monitored by a pair of PPACs placed in front of the Al foils during implantation. This experimental arrangement limited the total counting rate to 30 kps, but it was necessary as both the normal beam monitor setup (pin diodes mounted around the target), and the backup device (a fast plastic scintillator located at Image 1) failed to work during the experiment. The fragments were identified using the standard ΔE-Bρ-ToF method.

The data from the Si telescope detector are being processed, and a preliminary value of about

2.5×10^8 has been deduced for the total number of ^{108}Ag (2.4 min.) + ^{108m}Ag fragments that were implanted into the Al foil during a 24-hr bombardment. To verify results we produced an additional source which contained about half this number of fragments.

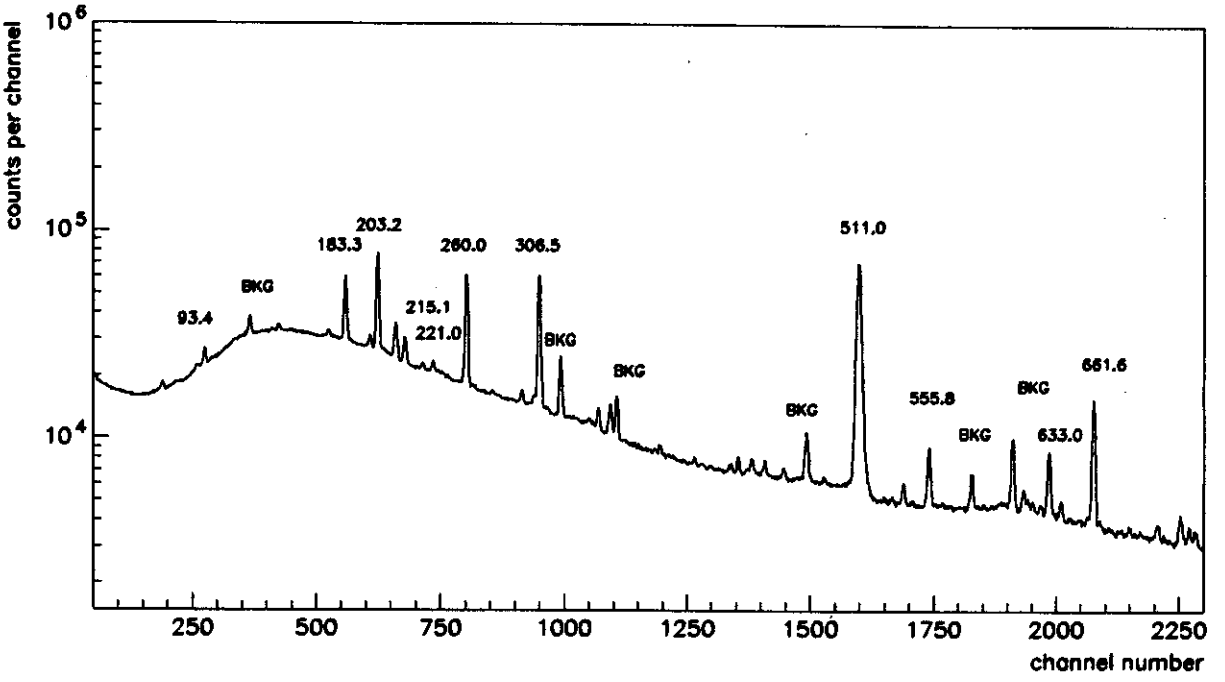

Figure 1. Partial γ-ray spectrum measured during implantation for about 24 hours. The 633.0-keV line is from ^{108}Ag(2.4 min.) decay. Identification of the other lines is as follows: 183.3 keV, ^{105}Pd (35 μs); 203.2 keV and 260.0 keV, ^{109}Cd(11 μs); 215.1 keV, ^{107}Pd(21 s); 221.0 keV, ^{101}Ru(17 μs); 306.5 keV, ^{105}Pd(35 μs) + ^{101}Ru(17 μs); 511.0 keV (mostly annihilation radiation); 555.8 keV, possibly ^{104}Ag(33.5 min.); 661.6 keV, possibly ^{113}Sn (86 ns); BKG, room background.

While the γ rays from ^{108m}Ag are being measured in a low-background facility at Berkeley Lab., additional data analysis done at MSU will provide values for the relative number of the various Ag isotopes that were implanted into the Al foil. These data, together with the known half-life values of the implanted Ag isotopes may be used to independently verify results for ^{108m}Ag.

a. Ernest Orlando Lawrence Berkeley National Laboratory, Berkeley, California

References

1. *Table of Isotopes*, 7th edition, C.M. Lederer and V.S. Shirley, editors; E. Browne, J.M. Dairiki, and R.E. Doebler, principal authors; A.A. Shihab-Eldin, L.J. Jardine, J.K. Tuli, and A.B. Buyrn, authors; John Wiley and Sons, Inc., New York (1978).
2. *Table of Radioactive Isotopes*, Edgardo Browne and Richard B. Firestone, authors; V.S. Shirley, editor; John Wiley and Sons, Inc., New York (1986).
3. *X-ray and gamma-ray standards for detector calibration*, Report IAEA-TECDOC-619, September 1991.
4. G. Harbottle, Radioch. Acta **13**, 132 (1970).
5. H. Vonach, M. Hille, and P. Hille, *Z. Phys.* **227**, 381 (1969).
6. U. Schotzig, H. Schrader, and K. Debertin, Proc. Intl. Conf. Nuclear Data for Science and Technology, Julich, Germany (1992), p. 562.
7. B.M. Sherrill et al., Nucl. Instr. Methods **B56**, 1106 (1991).